Visualization and Exploration of the Dynamics of Phase Slip Centers in Superconducting Wires

Iris Dorn[1], Armen Gulian [1,2]
1. Chapman University, Orange, CA USA
2. Chapman University, Institute for Quantum Studies, Advanced Physics Laboratory, Burtonsville, MD USA

Introduction

The dynamics of phase slip centers in a 1D model of superconducting wire was created based on the set of time-dependent Ginzburg-Landau equations (TDGL). COMSOL Multiphysics® General Form PDE interface was used. TDGL has successfully applied to this problem decades ago and most recently, the visibility of solutions has been enhanced by engaging COMSOL's power. The feature which distinguishes the current report here is that, for the first time, the set of TDGL equations for superconductors with finite gap was used in full. The terms relevant to the presence of finite gap were included not only into the equation for the wave function of the condensate, but also into the equation for the current in the form of interference terms.

The performed thorough study of the solutions of these non-linear equations required extensive searches for multiple solutions at certain values of given parameters. We found it extremely helpful using the built-in capability of COMSOL which could be operated in tandem with MATLAB®. By developing the MATLAB code, we were able to automate findings of the relevant solutions. We obtained "branching" and "anti-branching" of these solutions at certain parameters of the problem. These properties are directly relevant to experimental results being obtained with these objects.

Evolution of phase-slip centers takes place on picosecond time-scale, which can be very hard to visualize in practice. COMSOL's ability to generate animation provides unique opportunities to trace details of the microscopic evolution of various observables (such as the Cooper-pair density, superfluid and normal velocities, etc.). The most interesting cases and the most characteristic features will be demonstrated at the presentation as movies and they are available for downloading in link in the appendix.

Theory

Bardeen, Cooper and Schrieffer in the microscopic explanation of superconductivity[1] already proposed that the Ψ -function of the Ginzburg-Landau theory[2] at thermodynamic description of superconducting state may be related to the energy gap in the spectrum of paired electrons. Later this idea was proven by Gor'kov[3]. Increased efforts have been developed to generalize these microscopic equations for time-dependent problems, especially by Schmid[4] who came to the conclusion that the proper equation for the Ψ -function is not like the Schrödinger equation but rather had a diffusion character. This result was confirmed by Éliashberg and Gor'kov [5] on the basis of the Green's function model of superconductivity.

Interestingly, at that point a closed system of TDGL equations resulted for gapless superconductors[6] only. After the development of more powerful energy-integrated Green's function-based kinetic equations for non-equilibrium superconductivity, this system of equations in closed form was explicitly derived by other researchers[7-10]. In all of these attempts, the expression for current corresponding to the dynamics of superconductors was presented in the form which corresponds to the two fluid model of superconductivity[11].

As shown in Ref. 12, for superconductors with finite gap the microscopic theory yields additional terms in the current which corresponds to the interference between superconducting and normal motions of electrons. These terms could be essential in many situations. However, they have not been taken into account in a vast amount of research articles. We have included them into our framework of TDGL equations with a hope that this will be interesting for both researchers in various fields of physics and as well as for mathematicians, who are currently paying close attention to the properties of these non-linear set of equations.

Equations for Simulation

Let us consider the dynamic equation for the order parameter $\Delta = |\Delta|\, exp(\, i\theta)$:

$$-\frac{\pi}{8T_c}\frac{1}{\sqrt{1+(2\tau_\varepsilon|\Delta|)^2}}\left(\frac{\partial}{\partial t}+2i\phi+2\tau_\varepsilon^2\frac{\partial|\Delta|^2}{\partial t}\right)\Delta + \frac{\pi}{8T_c}[D(\nabla-2iA)^2]\Delta + \left[\frac{T_c-T}{T_c}-\frac{7\zeta(3)|\Delta|^2}{8(\pi T_c)^2}\right]\Delta = 0. \quad (1)$$

Here the theoretical units $\hbar = c = e = 1$ are used, A and ϕ are vector and scalar potentials of the electromagnetic field, T_c is the critical temperature of the superconductor, τ_ε is the electron-phonon relaxation time, D is the electronic diffusion coefficient, and $\zeta(3)$ is the Riemann zeta function.

Equation (1) describes the behavior of the Cooper pair condensate. The order parameter Δ ($|\Delta|$ is equal to the superconducting energy gap) is proportional to the original Ginzburg-Landau Ψ -function (normalized so as its squared modulus is equal to the density of pair condensate). One can obtain from (1) the "dirty metal" superconducting coherence length $\xi(T) = \{\pi D/[8(T_c - T)]\}^{\frac{1}{2}} \equiv \xi$.

Numerical modeling requires Eq. (1) in dimensionless form. This is done by dividing (1) by $\eta = (T_c - T)/T_c$, normalizing the order parameter by the relation $\Psi = \Delta/\Delta_0$ (where $\Delta_0 = \{8\pi^2 T_c(T_c - T)/[7\zeta(3)]\}^{\frac{1}{2}}$ is the equilibrium temperature-dependent value of the order parameter), and denoting $\delta = 2\tau_\varepsilon\Delta_0$, $\tau = \frac{tD}{\xi^2} \equiv \frac{t}{t_0}$ and $\bar{\phi} = \frac{2\phi\xi^2}{D} \equiv 2\phi t_0$.

After straightforward algebra we obtain equation

$$\frac{1}{\sqrt{1+\delta^2|\Psi|^2}}\left(\frac{\partial}{\partial\tau}+i\,\bar{\phi}+\frac{1}{2}\delta^2\frac{\partial|\Psi|^2}{\partial\tau}\right)\Psi = \xi^2(\nabla-2iA)^2\Psi + (1-|\Psi|^2)\Psi. \quad (2)$$

The vector potential as well as spatial derivatives in (2) are not yet normalized. Since in the Ginzburg-Landau approach another spatial parameter, the London penetration length, λ_L, comes in from the equation for the current density, j, then the final choice for the normalization of spatial derivatives will be done after considering that equation:

$$j = \frac{\pi\sigma_n}{4T}Q\left(|\Delta|^2-\frac{1}{\gamma}\frac{\partial|\Delta|^2}{\partial t}\right) + \sigma_n E\left\{+\frac{\sqrt{|\Delta|^2+\gamma^2}}{2T}\left[K\left(\frac{|\Delta|}{\sqrt{|\Delta|^2+\gamma^2}}\right) - E\left(\frac{|\Delta|}{\sqrt{|\Delta|^2+\gamma^2}}\right)\right]\right\}. \quad (3)$$

Here σ_n is the conductivity of normal excitations in superconductor, $\gamma = (2\tau_\varepsilon)^{-1}$, $K(x)$ and $E(x)$ are the complete elliptic integrals of the first and second type, respectively, $Q = -2A + \nabla\theta$, and $E = -\dot{A} - \nabla\phi$. Using the relations $curlH = 4\pi j = curlcurl\, A$, $u = \pi\text{^}4/[14\zeta(3)]$, $\eta = (T_c - T)/T_c$, and also choosing the gauge $\phi = 0$, we arrive, after some intermediate transformations, at the following equation for the current (3):

$$\sigma\dot{A}\left\{1+\frac{2}{\pi}\sqrt{\eta u}|\psi|\frac{\sqrt{(|\psi|\delta)^2+1}}{|\psi|\delta}\left[K\left(\frac{|\psi|\delta}{\sqrt{|\psi|^2\delta^2+1}}\right) - E\left(\frac{|\psi|\delta}{\sqrt{|\psi|^2\delta^2+1}}\right)\right]\right\} = -\left[A+\frac{i}{2\kappa|\psi|^2}(\psi^*\nabla\psi-\psi\nabla\psi^*)\right]\left(|\psi|^2-2\delta\sqrt{\frac{\eta}{u}}\frac{\partial|\psi|^2}{\partial\tau}\right) - \nabla\times\nabla\times A, \quad (4)$$

where $\sigma = \frac{\sigma_n}{t_0}$, $t_0 = \frac{\xi^2}{D}$.

In the same representation $\phi = 0$, equation (2) acquires the form:

$$\frac{1}{\sqrt{1+\delta^2|\Psi|^2}}\frac{\partial\Psi}{\partial\tau} = -\frac{\delta^2}{2\sqrt{1+\delta^2|\Psi|^2}}\frac{\partial|\Psi|^2}{\partial\tau}\Psi - [(\frac{i}{\kappa}\nabla + A)]^2\Psi + (1-|\Psi|^2)\Psi. \quad (5)$$

Here $\kappa = \frac{\lambda_L}{\xi}$ is the Ginzburg-Landau parameter, and $\lambda_L = \{8\pi^4\sigma_n(T_c - T)/[7\zeta(3)]\}^{-\frac{1}{2}}$.

For acceleration of numerical computations, it is convenient to replace the elliptic integrals in the expression (4) by elementary functions. With a good enough approximation, this could be done by the following relation:

$$K(x) - E(x) \cong \frac{ln(1+x) - ln(1-x)}{2} + (1-x)\,ln(1-x) \equiv \frac{ln(1-x^2)}{2} - x\,ln(1-x) \equiv f(x)/x. \quad (6)$$

It is not difficult to deduce that as $\delta \to 0$, Eq. (4) converts into the gapless expression

$$\sigma\dot{A} = -\left[A + \frac{i}{2\kappa|\psi|^2}(\psi^*\nabla\psi - \psi\nabla\psi^*)\right](|\psi|^2) - \nabla\times\nabla\times A, \quad (7)$$

In which case, interference terms do not matter. However, when $\delta \to \infty$, interference terms diverge. The latter is related with the case $\tau_\varepsilon|\Delta| \to \infty$, which is unphysical since the inelastic scattering rate of electrons is always finite. However, if $\tau_\varepsilon|\Delta| \geq 1$ then these interference terms[12] are essential for realistic description at modeling. It is worth noting that in equation for the Ψ -function, (1) or (2), similar contributions have been taken into account by many researchers since their introduction in Refs. 7-10. Thus our approach which takes into account finite values for for Ψ -function, and for δ, could be considered as logically consistent,

Numerical Model

To begin with COMSOL, we will replace with Log approximation function.

$$\sigma\dot{A}\left\{1 + \frac{2}{\pi}\sqrt{\eta u}|\psi| f\left(\frac{|\psi|\delta}{\sqrt{|\psi|^2\delta^2+1}}\right)\right\} = -\left[A + \frac{i}{2\kappa|\psi|^2}(\psi^*\nabla\psi - \psi\nabla\psi^*)\right]\left(|\psi|^2 - 2\delta\sqrt{\frac{\eta}{u}}\frac{\partial|\psi|^2}{\partial\tau}\right) - \nabla\times\nabla\times A, \quad (8)$$

Technical details of implementation into COMSOL Multiphysics® are discussed in Appendix.

Once the equation based modeling was fully implemented, with three general form PDE interfaces and Dirichlet Boundary conditions, the geometry was built as a simple 1 D wire of half-length L. The time-dependent solutions were simulated for given interval of time in seconds with time steps of 0.1. The parameters for the results were set to: $\sigma = 1, \kappa = 0.4, A_0 = 0, x_0 = 5, width = 0.1$ and $\eta = 0.5$.

The dynamics of time-dependent solutions were solved for by producing plots of the modulus of Ψ, $\sqrt{Re(\Psi)^2 + Im(\Psi)^2} \equiv \sqrt{u^2 + u_2{}^2}$, with respect to the x-coordinate. The parameters of j_0 and $\tau_\varepsilon|\Delta|$ were swept in search for the critical current, j_c, in which the first phase slip center occurs. This was accomplished through LiveLink™, which established a connection between COMSOL and MATLAB®, allowing MATLAB script via commands to control the COMSOL model. MATLAB script was created to automate sweeping through values of j_0 for select values of $\tau_\varepsilon|\Delta|$and discovering minima of prominence ≥ 0.996 in the modulus of Ψ. In turn, when the automation code located j_c for specific values of $\tau_\varepsilon|\Delta|$, these values were stored as well as the location of the PSC along the wire in datasets. Plots of these values of energy gap versus the critical current and the location of PSC at the critical current versus delta were generated and will be discussed in the next section. See Appendix for the MATLAB® automation code link.

Results of Finite Element Modeling

The behavior of PSCs in 1D wires have been extensively studied in the literature both experimentally[14] and theoretically[15]. Review articles and books are existent and interested readers can find references therein. As was mentioned in the Introduction, the interference terms in the current are dropped in almost all theoretical articles except some results[10]. However, no systematic research was performed even in Ref. 10. We will fill in this gap here by our studies, which will demonstrate the role of the finite gap in the dynamics of PSC in full extent (this factor will be included for Ψ -function and the current).

In Figure 1, we show the first phase slippages, which occurs when the density of pair condensate has a single touching at the center of the 1D wire, for different values of $\tau_\varepsilon|\Delta|$. Here we can see the tracing of the modulus of Ψ along the wire evolving over time, first bowing at the center until there is a very clear single dip to modulus of $\Psi = 0$. For $\tau_\varepsilon|\Delta|$= 0.1 & 0.6, the ends of the wire are unaffected by the phase slippage, while for $\tau_\varepsilon|\Delta|$ = 1.1 & 1.5, there is a decrease in modulus of Ψ at the ends and an overall increased bowing along the wire. It should also be noted that the increase in $\tau_\varepsilon|\Delta|$ also increases the time for the first phase slippage.

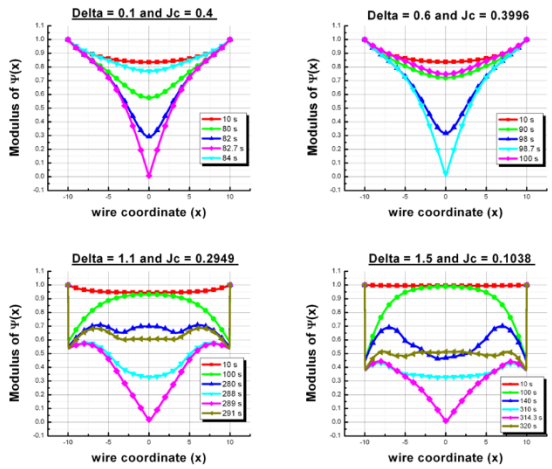

Figure 1. Set of single phase slippage along a 1D wire versus the modulus of Ψ (density of pair condensate), evolving over time for increasing $\tau_\varepsilon|\Delta|$.

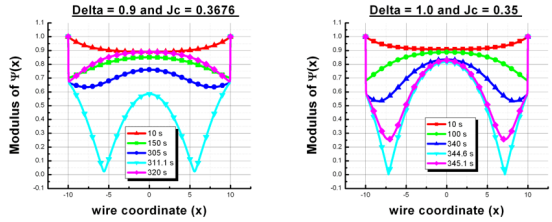

Figure 2. Set of double phase slippage evolving over time for increasing $\tau_\varepsilon|\Delta|$.

At and between $\tau_\varepsilon|\Delta| = 0.9$ and 1.0, we observe the double phase slippage evolving over time, with the low values of $\tau_\varepsilon|\Delta|$ in this region showing the double phase slippages closer to the center of the wire, while increasing the $\tau_\varepsilon|\Delta|$ in this region shows the double phase slippages moving away from the center and toward the ends of the wire.

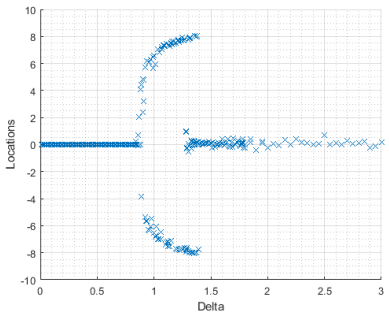

Figure 2. Location of PSCs with increased $\tau_\varepsilon|\Delta|$ with branching and anti-branching.

From these results, we obtained "branching" and "anti-branching" of $\tau_\varepsilon|\Delta|$ at their critical currents. The locations of the phase slippages versus $\tau_\varepsilon|\Delta|$ are plotted in Fig. 3.

Conclusion

These results demonstrate only a minor part of our findings, thanks to the power of COMSOL paired with MATLAB®. These two softwares combined have provided our research the exceptional ability to go into great details in regards to visualize and exploration of microscopic phenomena fine enough to be close to experimental findings. Future work includes modeling the time evolution of the current densities (interference, normal and superconducting), sweeping through the phonon term, and modeling the current in thin 2D films and massive 3D samples.

References

1. Bardeen, J.; Cooper, L. N.; Schrieffer, J. R. "Microscopic Theory of Superconductivity". *Physical Review*. **106** (1): 162–164. (1957)
2. Ginzburg, V.L. and Landau, L.D., *Zh. Eksp. Teor.Fiz.* **20**, 1064 English translation in: L. D. Landau, Collected papers (Oxford: Pergamon Press) p. 546.(1965)
3. Gorkov, L.P., *On the energy spectrum of superconductors*, Sov. Phys. JETP 7(3), 505-508 (1958).
4. Schmid, A. A time dependent Ginzburg-Landau equation and its application to the problem of resistivity in the mixed state. *Physik der kondensiertenMaterie*, *5*(4), 302-317. (1966)
5. Gor'kov, L.P. , Éliashberg, G.M., *Dynamical properties of gapless superconductors*, J. Low Temp. Phys., 2(2), 161-172, (1970)
6. Abrikosov, A. A., & Gor'kov, L. P. Contribution to the theory of superconducting alloys with paramagnetic impurities. *Zhur.Eksptl'.iTeoret. Fiz.*, *39*. (1960)
7. Golub, A. A. Dynamic properties of short superconducting filaments. *Zh. Eksp. Teor.Fiz*, *71*, 341. (1976)
8. Hu, C. R. Midgap surface states as a novel signature for d x a 2-x b 2-wave superconductivity. *Physical Review Letters*, *72*(10), 1526. (1994)
9. Watts-Tobin, R. J., Krähenbühl, Y., & Kramer, L. , Nonequilibrium theory of dirty, current-carrying superconductors: phase-slip oscillators in narrow filaments near Tc. *Journal of Low Temperature Physics*, *42*(5), 459-501. (1981)

10. Gulian, A. M., &Zharkov, G. F. *Nonequilibrium Electrons and Phonons in Superconductors*, Kluwer Academic/Plenum Publishers, New York, 1999.
11. Gorter, C. J., & Casimir, H., On supraconductivity I. *Physica*, *1*(1-6), 306-320. (1934)
12. A.M. Gulian, G.F. Zharkov, G.M. Sergoyan, Dynamics generalization of Ginzburg-Landau equations, in: L.V. Kedysh, V.Ya. Fainberg (Eds.), Problems of Theoretical Physics and Astrophysics, Nauka, Moscow, Chapter 10. (1989)
13. Kawamura, J., Chen, J., Miller, D., Kooi, J., Zmuidzinas, J., Bumble, B., ...& Stern, J. A. Low-noise submillimeter-wave NbTiN superconducting tunnel junction mixers. *Applied Physics Letters*, *75*(25), 4013-4015. (1999).
14. Michotte, S., Mátéfi-Tempfli, S., & Piraux, L., 1D-transport properties of single superconducting lead nanowires. *Physica C: Superconductivity*, *391*(4), 369-375. (2003)
15. Eggel, T., Cazalilla, M. A., & Oshikawa, M., Dynamical theory of superfluidity in one dimension. *Physical review letters*, *107*(27), 275302. (2011)

Acknowledgements

We are grateful to G. Melkonyan for helpful discussions, and J. Tollaksen for encouraging our TDGL modeling. This work was supported in part by ONR Grants N00014-16-1-2269, N00014-17-1-2972, N00014-18-1-2636, and N00014-1901-2265.

Appendix

The Equation Based Modeling with the Partial Differential Equation (PDE) interface was utilized in COMSOL for this simulation. Equation 6 required one replacement before implementing into the program, $u = \frac{\pi^4}{[14\zeta(3)]} \cong 5.798$ since the term u is also used for the PDE interface. After this replacement, the real and imaginary parts of the order parameter are represented as $Re(\psi) = u(x,t)$ and $Im(\psi) = u_2(x,t)$ with u, u_t, u_x and u_{xx} denotes partial derivatives with respect to x or t and the subscript of the variable (u,u_2,u_3,...).

The form of the PDE to be solved is: $\boldsymbol{e}_a \frac{\partial^2 u}{\partial t^2} + d_a \frac{\partial u}{\partial t} + \nabla \cdot \Gamma = F$ and this form was used three times. The first PDE interface (PDE_1) is for the real part of ψ, the second (PDE_2) is for the imaginary part of ψ, and the third (PDE_3) is for the vector potential, A. For all three PDE forms, $\boldsymbol{e}_a$=0. The values of d_a for PDE_1 and PDE_2 are set to 1, while PDE_3 has this value defined by:

$$d_a = \sigma\left(1 + (1/\pi)(5.798 \cdot \eta(u^2 + u_2{}^2))^{\frac{1}{2}}(exact[\frac{1}{\left(1+\frac{1}{(u^2+u_2{}^2)\Delta^2)^{\frac{1}{2}}}\right]})\right),$$

where $exact$ is an interpolated function defined in the set of Global Definitions from a data set. Equivalently for this analytic function, we also used an interpolated function, a feature of the COMSOL Global Definitions, by uploading a data set of the difference of the elliptic functions.
The expressions for terms Γ and F for each PDE are as follows:

$PDE_1: \Gamma_1 = -\frac{u_x}{\kappa^2}$,

$$F_1 = -\frac{u_{xx}}{\kappa^2} + \frac{\left((1+\Delta^2 u_2{}^2)u_{xx}\right)}{\left(\kappa^2\sqrt{1+\Delta^2(u^2+u_2{}^2)}\right)} - \frac{(\Delta^2 u u_2 u_{2xx})}{\left(\kappa^2\sqrt{1+\Delta^2(u^2+u_2{}^2)}\right)} + \frac{\left(2u_{2x}(1+\Delta^2 u_2{}^2)(u_3+A_0)\right)}{\left(\kappa\sqrt{1+\Delta^2(u^2+u_2{}^2)}\right)} + \frac{\left(2u_x\Delta^2 u u_2(u_3+A_0)\right)}{\left(\kappa\sqrt{1+\Delta^2(u^2+u_2{}^2)}\right)} + \left(\frac{u_2 u_{3x}\left(\sqrt{1+\Delta^2(u^2+u_2{}^2)}\right)}{\kappa}\right) - \left(u(u_3+A_0)^2/\left(\sqrt{1+\Delta^2(u^2+u_2{}^2)}\right)\right) + \frac{u(1-u^2-u_2{}^2+p(((x-x_0)/2)^2<width))}{\left(\sqrt{1+\Delta^2(u^2+u_2{}^2)}\right)}$$

$PDE_2: \Gamma_2 = -\frac{u_{2x}}{\kappa^2}$

$$F_2 = -\frac{u_{2xx}}{\kappa^2} + \frac{\left((1+\Delta^2 u_2{}^2)u_{2xx}\right)}{\left(\kappa^2\sqrt{1+\Delta^2(u^2+u_2{}^2)}\right)} - \frac{(\Delta^2 u u_2 u_{xx})}{\left(\kappa^2\sqrt{1+\Delta^2(u^2+u_2{}^2)}\right)} - \frac{\left(2u_x(1+\Delta^2 u^2)(u_3+A_0)\right)}{\left(\kappa\sqrt{1+\Delta^2(u^2+u_2{}^2)}\right)} - \frac{\left(2u_{2x}\Delta^2 u u_2(u_3+A_0)\right)}{\left(\kappa\sqrt{1+\Delta^2(u^2+u_2{}^2)}\right)} - \left(\frac{u u_{3x}\left(\sqrt{1+\Delta^2(u^2+u_2{}^2)}\right)}{\kappa}\right) - \left(u_2(u_3+A_0)^2/\left(\sqrt{1+\Delta^2(u^2+u_2{}^2)}\right)\right) + \frac{u_2(1-u^2-u_2{}^2+p(((x-x_0)/2)^2<width))}{\left(\sqrt{1+\Delta^2(u^2+u_2{}^2)}\right)}$$

And $PDE_3: \Gamma_3 = 0$

$$F_3 = -(u_3+A_0)\left(u^2+u_2{}^2 + 2\Delta a_{11}(2uu_t + 2u_2 u_{2t})\right) + \left(\frac{uu_{2x}-u_2 u_x}{\kappa}\right)\left(1 + 2a_{11}\left(\frac{\Delta}{u^2+u_2{}^2}\right)(2uu_t + 2u_2 u_{2t})\right) - j_0$$

Here $a_{11} = \sqrt{\frac{\eta}{5.798}}$.

The conditions at the ends of the wire were controlled by Dirichlet boundary conditions of zero flux ($\boldsymbol{n} \cdot \Gamma = 0$). However, each PDE interface has different prescribed values, r, of their respective Dirichlet boundary conditions, $r_1 = 1$, $r_2 = 0$, and $r_3 = -j_0 - A_0$. In additional, initial values must be applied for each PDE interface:
PDE_1 has $u = 1$ and $\frac{du}{dt} = 0$, PDE_2 has $u_2 = 0$ and $\frac{du_2}{dt} = 0$, and PDE_3 has $u_3 = -j_0 - A_0$ and $\frac{du_3}{dt} = 0$.
Of great important to adequate solutions of this set of PDEs is a custom Mesh setting with maximum

element size = 0.01, maximum element growth rate = 1 and resolution of narrow regions = 1.

To view or download the MATLAB® automation code, go to https://irisdorn.github.io/automatedcomsol/.